Pergamon

Geochimica et Cosmochimica Acta, Vol. 68, No. 8, pp. 1777–1789, 2004

0016-7037/04 $30.00 + .00

doi:10.1016/j.gca.2003.10.005

U and Th concentrations and isotope ratios in modern carbonates and waters from the Bahamas

Laura F. Robinson,* Nick S. Belshaw, and Gideon M. Henderson
Department of Earth Sciences, Oxford University, Parks Road, Oxford OX1 3PR, United Kingdom

(*Received February* 11, 2003; *accepted in revised form October* 15, 2003)

Abstract—The short residence times of Th and Pa in seawater make them very responsive to changes in the ocean environment. We use a new multi-ion-counting technique to make Th and Pa isotope measurements in seawaters from a near-shore environment in which oceanic chemical tracers are not overwhelmed by terrestrial inputs (the Bahamas). An unusual feature of the Bahamas setting is the shallow depth of water residing on the bank tops. These waters have significantly lower $^{232}Th/^{230}Th$ (~10,000) than those immediately adjacent to the banks (24,000–31,000) and a ($^{231}Pa/^{230}Th$) near the production ratio (~0.1). The change in $^{232}Th/^{230}Th$ and ($^{231}Pa/^{230}Th$) on the bank tops is explained by almost quantitative removal of Th and Pa by scavenging, and their replacement with a mixture of ^{230}Th and ^{231}Pa alpha-recoiled from the underlying carbonates, together with Th from dust dissolution. Analysis of a water profile in the Tongue of the Ocean, which separates the Great and Little Bahama Banks, allows us to trace the movement of bank-top water to depth. A distinct minimum in both $^{232}Th/^{230}Th$ (~13,000) and ($^{231}Pa/^{230}Th$) (~0.5) is observed at ~430 m and is interpreted to reflect density cascading of bank-top water with entrained carbonate sediment. These results suggest that Th and Pa can be used as water-mass tracers in near-shore environments. Uranium concentration measurements on the same waters demonstrate that U is conservative across a range in salinity of 2 psu, with a concentration of 3.33 ppb (at a salinity of 35).

The incorporation of U and Th isotopes into marine carbonates has also been assessed by analyzing carbonate samples from the same location as these Bahamas waters. Such incorporation is critical for U-Th geochronology. U isotope analyses demonstrate that seawater $\delta^{234}U$ averages 146.6 and does not vary by more than 2.5‰, and that carbonates capture this value. Additional high precision measurements (≈±1‰) on modern carbonates confirm that all oceans have identical $\delta^{234}U$. Modern marine carbonates are shown to have $^{232}Th/^{230}Th$ ratios that reflect the local seawater in which they formed. *Copyright © 2004 Elsevier Ltd*

1. INTRODUCTION

This study has two distinct goals: to understand more fully the incorporation of U and Th isotopes into marine carbonates when they form; and to assess the controls on Th and Pa isotopes in seawater in the near-shore environment.

The U isotope ratio ($^{234}U/^{238}U$) is frequently used in marine carbonates to test for diagenesis and open-system behavior during U/Th dating. This approach makes the inherent assumption that marine carbonates incorporate U at the same isotope ratio as seawater. In fact, there have been remarkably few high-precision studies of ($^{234}U/^{238}U$) in seawater. The first measurements by thermal ionization mass spectrometry (TIMS, Chen et al., 1986) suggested a ratio of 1.140 (after adjustment for the new half-life of Cheng et al., 2000a, as used throughout this paper). These measurements had an uncertainty of some 4‰ (Fig. 1). In contrast, high precision ($^{234}U/^{238}U$) measurements on recent corals are more numerous and have an average of 1.146 (±1.7‰) (n = 22; Cheng et al., 2000a; Fig. 1). Measurements on modern carbonates other than corals have not been made at high precision. The uncertainties in seawater and carbonate ($^{234}U/^{238}U$) measurements allow for the possibility that carbonates form with slightly higher ($^{234}U/^{238}U$) than seawater, or gain this higher ratio immediately after death. Indeed, some workers have suggested higher ($^{234}U/^{238}U$) in modern corals as a result of very early reef diagenesis, and that this increase in ratio may be part of the same process that leads to high ($^{234}U/^{238}U$) in many older corals (Lazar et al., 2002). No study has systematically tested the incorporation of ($^{234}U/^{238}U$) into marine carbonates by coupled seawater and carbonate measurements from the same location. Investigating the incorporation of U isotopes into carbonates is the first objective of this study. Throughout the rest of this paper, the ratio ($^{234}U/^{238}U$) will be expressed as $\delta^{234}U$ ($=[\{(^{234}U/^{238}U)_{meas}/(^{234}U/^{238}U_{eq})\} - 1] \times 10^3$).

Ideally, marine carbonates have negligible initial Th and therefore do not require correction for nonzero initial $^{230}Th/^{238}U$. Many carbonates do not fit this ideal, with a notable example being the aragonite sediments found on the slopes of the Bahamas (Slowey et al., 1996; Henderson et al., 2001; Robinson et al., 2002). Such "dirty" carbonates require a correction for initial Th, which is generally performed using an assumed initial $^{232}Th/^{230}Th$. For continental carbonates, a typical crustal $^{232}Th/^{230}Th$ is normally used (e.g., Ludwig and Paces, 2002), but this correction is unlikely to be valid for marine samples which may incorporate either detrital material with a high $^{232}Th/^{230}Th$, or seawater Th with a low $^{232}Th/^{230}Th$ (Henderson et al., 2001). No study has systematically assessed the incorporation of Th isotopes into marine carbonates by coupled measurements from the same location. Such a study is important if U/Th ages from "dirty" marine carbonates are to be reliably corrected for initial Th. Assessing the incorporation of

* Author to whom correspondence should be addressed, at Division of Geological and Planetary Sciences, California Institute of Technology, MS 100-23, 1200E California Boulevard, Pasadena, CA 91125, USA (laurar@gps.caltech.edu).

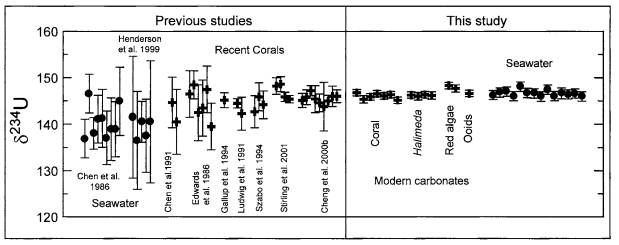

Fig. 1. $\delta^{234}U$ in water and modern carbonates. Circles are from seawater and crosses are from modern and recent carbonates including samples of coral, *Halimeda*, red algae and ooids. Errors are 2 s.e.

thorium isotopes into marine carbonates is the second objective of this study.

The factors that control Th isotopes in the near-shore environment can also be investigated by making high precision analyses. Coupled ^{231}Pa analyses allow us to observe variability in Th and Pa concentrations, as well as the $^{232}Th/^{230}Th$ and $^{231}Pa/^{230}Th$ ratios. Significant work has been performed on these geochemical tracers in the open ocean (e.g., Anderson et al., 1983; Moran et al., 2001), and has demonstrated their power as proxies for ocean circulation, sedimentation rates, and past ocean productivity (e.g., Henderson and Anderson, 2003). Considerably less work has been performed in the near-shore environment (Anderson et al., 1983; Anderson et al., 1990). No study has investigated the processes that set these geochemical tracers in a shelf or bank environment, nor their potential uses in such an environment. This investigation is the third objective of this study.

2. SAMPLE SELECTION AND REGIONAL SETTING

To investigate the behavior of Th isotopes as a tracer of near-shore processes, a series of 4–5-L water samples were collected in March 2001. A depth profile spanning the depth range 6 to 1650 m from The Tongue of the Ocean (TOTO, 25° 00.80 N 77°41.24 W, Fig. 2) was sampled sequentially using a single precleaned 10-L Niskin bottle. Samples were also collected just after high tide from Exuma Sound at 0, 10 and 20 m water depths and from the top of the Great Bahama Bank (GBB) (Fig. 2).

The Bahamas are situated in the western Equatorial Atlantic within the western boundary current. The NW and NE Providence Channels separate the Little Bahama Bank (LBB) and GBB (Fig. 2). Two deep channels, the TOTO (>4,000 m water depth) and Exuma Sound (~2000 m water depth) form areas of large topographic relief within the GBB. Salinity and temperature data show that water in the Providence Channels is predominantly from the Sargasso Sea and flows westwards into the Straits of Florida (Slowey and Curry, 1995). The thermocline in this region extends to approximately 1000 m (Slowey and Curry, 1995) and its upper portion is composed of North Atlantic Central Water (NACW) from the Sargasso Sea. Deep water (~1000–2000 m) is similar to that on the east of the LBB and consists of Labrador Sea type water.

Surface water on the LBB and GBB is subject to intense evaporation and becomes highly saline (>40, Morse et al., 1984; Whitaker and Smart, 1990). Water moves to the edge of the bank where it can sink as a dense plume and spread out at a depth of neutral buoyancy (Wilson and Roberts, 1992, 1993, 1995). The estimated depth to which it sinks varies from as shallow as 50 m (Hickey et al., 2000) to as deep as 800 m (Wilson and Roberts, 1995). The bank tops generate vast quantities of carbonate. The exact mechanism by which this carbonate is transported to the deeper slopes is not clearly understood. Wilson and Roberts (1995) suggest that dry air associated with the arrival of a cold front can enhance evaporation while cooling the water to produce very dense water. Vigorous wind and wave action entrains sediment from the bank top before the water flows down-slope to a depth of neutral buoyancy, a process they name density cascading. The modelled density gives a maximum depth of neutral buoyancy of between 450–800 m. Wilber et al. (1993) present field data supporting the presence of density cascades, but suggest that the currents are erosional rather than depositional.

The fast flowing water in the Straits of Florida to the west of the Bahamas moves northwards to form an effective barrier between the Bahamas and Florida (Fig. 2). This current prevents terrestrial material from reaching the Bahamas so the platform sediments are almost pure carbonate. Biogenic carbonate samples (coral, green algae and red algae) were collected in the vicinity of Lee Stocking Island to test the incorporation of U and Th isotopes into modern sediments (see Fig. 2 for localities). The combination of water and carbonate samples allows the incorporation of Th and U isotopes into carbonates to be understood. To expand this study, a limited number of samples were also collected from the Indian and Pacific Oceans.

3. CHEMICAL PROTOCOLS

3.1. Chemical Pretreatment of Samples

Each water sample was weighed (± 0.1 g), acidified to pH 2, spiked with a ^{236}U-^{229}Th mixed spike and left to equilibrate for

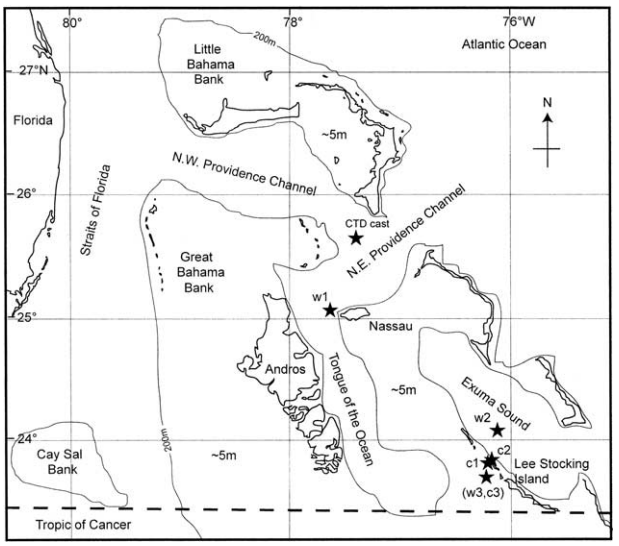

Fig. 2. Map showing localities of Bahamas samples. Thick black lines delimit land above sea level; thin black line delimits the 200 m contour at the edge of the two shallow banks. Symbols w1–3 are the three sites from which water samples were collected. Sites c1 and c2 are carbonate-sample sites from the lee and windward sides of Lee Stocking Island respectively. Site c3 is the ooid shoal.

Table 1. Collector array on the Nu Instruments MC-ICP-MS.[a]

	F(+7)	F(+5)	F(+3)	F(+2)	F(+1)	AXIAL	F(−1)	F(−2)	IC(−3)	F(−4)	IC(−5)	F(−6)	IC(−7)	F(−8)
Step 1			^{238}U		^{236}U	^{235}U	^{234}U		^{232}Th		^{230}Th			
Step 2				^{238}U		^{236}U	^{235}U	^{234}U	^{233}Pa		^{231}Pa		^{229}Th	

[a] The Axial and "F" collectors are Faradays. The three IC channels are ion counters. Numbers refer to the number of mass units away from the Axial collector, negative are on the low mass side and positive are on the high mass side. The second and third rows show the two-step run configuration used for measuring Th and Pa in seawater. Beams are counted for 10 s on each step

6 weeks. Spike U concentration is known from calibration against a certified gravimetric standard supplied by the New Brunswick Laboratory (CRM-145). Spike Th-concentration is known by calibration against a uraninite which is known to be close to secular equilibrium (Harwell-Uraninite-HU-1, with a (^{230}Th/^{238}U) 1.3‰ from secular equilibrium; Cheng et al., 2000a). A ^{237}Np-derived ^{233}Pa spike was added 24 h before U, Th and Pa coprecipitation with Fe oxyhydroxide. This Pa spike was provided through cooperation with S. Turner at Bristol University. The precipitate was rinsed in pure water, centrifuged, dissolved in concentrated HNO_3 and evaporated to dryness.

Organic material was removed from modern carbonates with either hot, concentrated hydrogen peroxide or by heating in an ashing furnace for ~30 h at 420°C. Samples were spiked using the ^{236}U-^{229}Th mixed spike and dissolved in 7.5 N HNO_3. Concentrated HNO_3 was added and the resulting solution evaporated to dryness to remove any remaining organic matter.

3.2. Column Chemistry

Separation of U and Th-Pa from the Fe fraction followed Edwards et al. (1986). Samples were loaded onto 2 mL anion exchange columns in 7.5 N HNO_3. Th and Pa were eluted with a mixture of 6 N HCl plus a trace of HF, followed by elution of uranium with H_2O.

^{233}Pa decays to its daughter ^{233}U with a half-life of 26.97 d, so the ^{233}Pa spike rapidly becomes a mixture of ^{233}Pa and ^{233}U. Both of these isotopes are ionized efficiently by plasma, so it is important to ascertain how much ^{233}U leaks into the Th-Pa fraction during chemistry to obtain accurate ^{231}Pa concentrations. The percentage of uranium remaining in the thorium fraction was calculated by adding a pure ^{236}U spike after column chemistry. The ^{238}U/^{236}U measured before (in the U fraction) and after the addition of the second spike allowed the yield of U in the Th-Pa fraction to be calculated. On average, less than 0.9% of the uranium entered the Th-Pa fraction.

3.3. Blanks

Seawater Th and Pa concentrations are low, so laboratory blank is frequently a major contribution to uncertainty (e.g., 15–100%; Cochran et al., 1995). Column chemistry ^{232}Th blank was 2 pg and ^{230}Th was below the detection limit. Full procedural blank for water samples was 48 pg for ^{232}Th and 2 fg for ^{230}Th. Both of these are approximately 10% of the total thorium content and are used to correct the final values. The ^{238}U blank was ~100 pg which is negligible. Pa-231 has a blank of 9 fg which is ~30% of the total sample size. Unlike ^{230}Th, this level of blank ^{231}Pa is higher than expected from the U blank (assuming secular equilibrium) suggesting a small amount of Pa contamination in one of the reagents. Results for all elements are corrected for blank, and the error propagated by assuming a 20% uncertainty on the blank correction.

4. MASS SPECTROMETRY

4.1. Previously Published Methods of Analysis

Both ^{230}Th and ^{231}Pa are scarce in seawater (~5 fg/kg at the surface) so large samples and/or sensitive instrumentation are needed for precise analyses. Originally, α-counting techniques gave a precision of 5–15% on sample volumes of >1000 L (e.g., Bacon and Anderson, 1982; Nozaki and Yamada, 1987; Nozaki and Yang, 1987; Nozaki et al., 1987). Guo et al. (1995) report similar precision using secondary ionization mass spectrometry. Thermal ionization mass spectrometry (TIMS) methods developed by Edwards et al. (1986) improved the precision. TIMS has subsequently been used in a number of studies with a typical precision of 5% on ^{230}Th (e.g., Banner et al., 1990; Andersson et al., 1995; and Roy-Barman et al., 1996). ICP-MS has allowed such measurements to be made even more precisely. Luo et al. (1997) first used double focussing multi-collector-ICP-MS to measure high precision ^{232}Th/^{230}Th ratios. Shen et al. (2002) describe a similar method using single-collector-ICP-MS which achieves 0.5% precision on ~400 fg of ^{230}Th, equivalent to 80 L of surface seawater. Single-collector-ICP-MS concentration measurements for ^{230}Th and ^{231}Pa have recently been reported at 2% for 10–20 L of deep water (Choi et al., 2001).

4.2. Instrumentation and Machine Configuration

In this study, MC-ICP-MS analyses were performed by aspirating U and Th through a Cetac Aridus nebulizer into a double-focussing Nu Instrument (Belshaw et al., 1998). The collector array includes twelve Faraday collectors (with 10^{11} MΩ resistors) and three ion counters, each consisting of an ETP electron multiplier. These ion-counters (IC) are situated at 3, 5, and 7 amu below the Axial Faraday collector when at mass 238 (Table 1). For the purposes of this paper all collectors will be referred to by their type (F or IC) and their mass relative to the Axial Faraday e.g., the ion counters are IC(−3), IC(−5) and IC(−7). IC(−5) is fitted with a retardation filter to improve abundance sensitivity. This ion-counter configuration allows multiple beams to be collected simultaneously, thus increasing the total number of ions collected and removing the uncertainty due to plasma noise (Table 1). Deadtime on the electron multipliers has been assessed as 23 ns by measuring the U standard,

Table 2. Typical beam sizes for key Th and Pa isotopes, together with a summary of error analysis for these isotopes.[a]

	Thorium 230			Thorium 232			Protactinium 233			Protactinium 231		
	12			240,000			70			30		
Typical beam size (cps)	% of signal	% uncert. on corr.	2% error	% of signal	% uncert. on corr.	2% error	% of signal	% uncert. on corr.	2% error	% of signal	% uncert. on corr.	2% error
Correction												
Blank	8.0	20	3.2	11	20	4.4				25	20	10.0
Memory	0.5	20	0.2	0.02	20	0.0	0.2	10	0.0	0.1	20	0.1
Ab. sensitivity	1.0	16	0.3				58	16	19.0	0.8	16	0.3
Hydrides							10	10	2.0			
Error from spike												22.4
Internal Error			6.0			1			12			12
Spike Calibration			1.6			1.6			3			4
Counting statistics			3.5			0.03			1.8			2.4
Total 2% error			7.0			4.8			22.4			27.6

[a] For the error analysis, the first column for each isotope is the proportion of the total beam that is due to the correction; the second is the uncertainty on that correction and the last column is the 2 s.e. percentage uncertainty on the final number. As described in the text the corrections which have a significant uncertainty are the blank, machine memory, abundance sensitivity and hydride formation. Additional errors come from the internal machine error, the spike calibration and, when calculating the ^{231}Pa, the uncertainty on the ^{233}Pa measurement. The average final error is the rms of all of these error sources. Counting statistics are given for comparison.

U-500, at varying intensities. Ion yields for uranium and thorium are better than 1‰.

4.3. Uranium

Uranium was run statically with ^{238}U, ^{236}U, and ^{235}U in Faraday collectors, and ^{234}U in IC(−3) following Robinson et al. (2002). Generally two sets of 45 10-s integrations were collected for waters, and three sets of 45 for carbonate samples at a ^{234}U intensity of $\sim 2\times10^4$ cps.

4.4. Thorium and Protactinium in Water Samples

Surface seawater samples of 4.5 kg contain only ~450 pg ^{232}Th, ~25 fg ^{230}Th and ~40 fg ^{231}Pa and are, therefore, best measured by ion counting. A two-step run configuration was used to collect up to 30 ratios with an integration time of 10 s on each step. This collection is summarized in Table 1 and involves ion-counting of ^{230}Th, ^{232}Th, ^{231}Pa and ^{233}Pa while larger U beams are monitored in Faradays. There are six important considerations when measuring such small samples by MC-ICP-MS: 1) plasma noise, 2) mass fractionation, 3) Faraday/ion-counter gain, 4) machine memory, 5) hydride formation and 6) abundance sensitivity. The uncertainty on each of these corrections is summarized in Table 2. Most of these corrections were assessed using the CRM-145 standard (also known as NBS-960 or CRM 112A) which has natural ^{238}U/^{235}U, and δ^{234}U slightly below secular equilibrium.

Plasma noise between the two steps was normalized using the large ^{238}U beam. If this correction is not applied then ratios remain accurate but are less precise. Incomplete U-Th separation during chemistry enabled ^{238}U/^{235}U monitored within the run to provide an internal correction for mass discrimination. The correction is made for each individual ratio and the uncertainty is negligible. A small difference between U and Th mass fractionation during plasma ionization has been reported at ~0.3‰ per amu (Pietruszka et al., 2002). At the level of precision reported in this study such differences are not significant. Gain was measured before and after each complete set of sample runs by measuring ^{238}U/^{235}U in a dilute solution of CRM-145 with the ^{235}U beam in IC (−3), (−5) and (−7) in turn. The gains vary by less than 0.2‰ during a day so the uncertainty on this correction in negligible.

Machine memory was minimized by ensuring that no concentrated thorium solutions were run immediately before water measurements, that clean cones were used and by washing for several hours with alternate 3 min washes of 2 and 10% HNO_3. Similar washes were carried out over 1 h between each sample. Machine memory that could not be removed by repeated washing was monitored by measuring each isotope in 2% HNO_3.Typical count rates for the memory were 0.2 cps on ^{230}Th and 0.1 cps on ^{231}Pa (compared to dark noise of the ion counters of ≈0.1 cps). All thorium and protactinium beams are corrected for machine memory. The uncertainty introduced from memory correction is small, the largest is a 0.2% (2σ) contribution to ^{230}Th uncertainty (Table 2), nevertheless the errors were propagated for each isotope.

The magnitude of Th-hydride formation was assessed by monitoring the 233 amu beam on a pure ^{232}Th solution in IC(−3), IC (−5) and IC (−7) with ^{232}Th in F(−4), F(−6) and F(−8) respectively. The beam at 233 amu, corrected for the contribution from abundance sensitivity, was 16 ppm of the ^{232}Th beam as measured in all three ion counters and on two different days, similar to the 14 ppm measured by Choi et al. (2001). This proportion corresponds to ~10% of the total 233 beam during sample analysis. The 2σ uncertainty due to this correction is 2%.

Abundance sensitivity was assessed in all three ion-counting channels over a range of mass separations by switching an 8-V ^{232}Th beam across all the Faraday collectors and monitoring the residual beam in each ion counter (Fig. 3a). Within 3 amu of ^{232}Th, the abundance sensitivity follows an exponential decrease with mass, as expected. At greater distances, the decrease of abundance sensitivity is not so rapid and the ^{232}Th tail extends at least 6 amu from the beam on the low mass side.

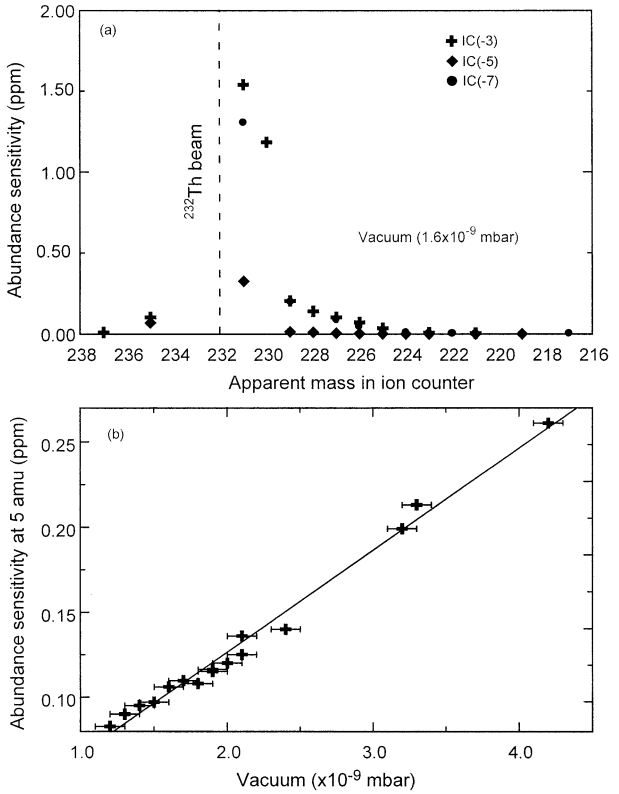

Fig. 3. Abundance sensitivity of the Nu Instrument. a) The ^{232}Th tail measured in each of the three ion counters at a vacuum of 1.6×10^{-9} mbar. Note that ion counters IC(−3) and IC(−7) do not have retardation filters and are in general agreement. IC(−5) has a retardation filter and shows significantly better abundance sensitivity. Missing data represent masses where measurement is made difficult by the two-mass-unit spacing of the ion counting channels. b) The abundance sensitivity at 233 amu measured in IC(−3) at a variety of vacuum states. The signal includes the tail from ^{238}U, ^{235}U and ^{234}U but is dominated by that from ^{238}U. As expected there is a linear relationship between abundance sensitivity and vacuum. This relationship has a scatter of ~8% (1 s.d.).

Since it is fitted with a retardation filter the abundance sensitivity for IC(−5) is low and is 0.3 ppm at 1 amu and ~0.01 ppm at 3 amu. The measurements of ^{231}Pa and ^{230}Th are therefore not significantly affected by the tail of the ^{232}Th beam. The most significant potential problem created by the abundance sensitivity is that from ^{238}U on ^{233}Pa, which is measured on IC(−3). Abundance sensitivity at −5 amu was therefore assessed more carefully, both for its variation with beam size and with changing vacuum conditions.

CRM-145 with a ^{238}U beam intensity of 1–6 V was used to assess the contribution of abundance sensitivity to the signal intensity at 233 amu. The abundance sensitivity is constant with increasing beam intensity and therefore can be calibrated at a single intensity before each sample set to correct measured beams.

The abundance sensitivity from ^{238}U at 233 amu was measured over 2 months to assess the external repeatability and the variability with fluctuating vacuum (Fig. 3b). With normal operating conditions the abundance sensitivity increases linearly as the vacuum deteriorates. These measurements were made whilst the vacuum could only be recorded digitally with a stepwise resolution of 0.1×10^{-9} mbar. A portion of the scatter about a linear relationship is due to uncertainty in the vacuum measurement. Nevertheless the scatter about the line is only 8%. The flight tube vacuum is normally between 1 and 3×10^{-9} mbar. Immediately before this study a focus plate problem required work inside the machine so the vacuum was somewhat worse than normal at 6×10^{-9} mbar. To account for this vacuum a conservative estimate of twice the typical uncertainty was used when propagating errors. For future analyses performed with more typical vacuum conditions this correction will be reduced leading to more precise isotope ratios.

The effect of abundance sensitivity was considered for all isotopes but only contributed a significant proportion of the beam for ^{230}Th, ^{231}Pa and ^{233}Pa. ^{230}Th and ^{231}Pa were measured in IC(−5) and so the contribution to the raw voltage from abundance sensitivity is small, ~1%. However, the magnitude of the abundance sensitivity measured in IC(−3) is of the same order as the expected ^{233}Pa beam in samples (Table 2). The final error associated with abundance sensitivity on ^{233}Pa is ~19%, which is about two thirds of the total error. This uncertainty can be dramatically improved in future studies by more thorough separation of U from Pa.

5. RESULTS

Uranium isotope ratios have been measured with a total precision of better than 1‰. δ^{234}U is constant through the Bahamas water column and has a range of 145.9 to 148.0, with an average of 146.3. Similarly, the eleven different modern carbonates display a δ^{234}U range of 145.1 to 148.3 with an average of 146.4 (Fig. 1). For both water and carbonates, three samples were replicated to check reproducibility of results, in each case the values were within analytical uncertainty.

Uranium-238 concentrations in the water column range from 3.40 to 3.56 μg/kg, the highest being from the bank top (Table 3, Fig. 4). The concentration tends to decrease from the surface down to 950 m with maxima at 120 m and 580 m. The concentration then increases at depth. Replicate samples are within analytical uncertainty. As expected, the uranium concentration in carbonates varies from species to species: corals from 2.16 to 3.11 ppm, *Halimeda* from 1.44 to 2.15 ppm, and both *Millipore* and Red algae have low concentrations of 0.31 and ~0.55 ppm respectively. Ooids have the highest concentration, 4.10 ppm (Table 3).

Water column ^{232}Th concentrations display subtle variations but are generally between 89 and 107 pg/kg with the exception of the 20 m sample in Exuma Sound which has a concentration of 136.7 pg/kg. The ^{230}Th concentrations show a distinctive structure with depth. Low values of 3–4 fg/kg are seen in near-surface waters, this rises to a peak of ~7.5 fg/kg at 580 m and falls again to 4.25 fg/kg at 1650 m. The bank-top sample has the highest concentration of 8.7 fg/kg. The ^{230}Th concentration structure is reflected in the ^{232}Th/^{230}Th ratio, with high values (>30,000) in surface waters, low values (13,000–14,000) at 400–500 m and then high values again (24,000) at 1650 m. Bank-top water ^{232}Th/^{230}Th is low (~10,500) reflecting the high ^{230}Th concentration. Three samples were replicated and are identical within analytical uncertainty.

The carbonate samples show a wide range in thorium con-

Table 3. Concentrations and isotopes ratios for all samples.[a]

	Locality	^{238}U (ppm)	2 s.e.	δ^{234}U (‰)	2 s.e.	^{232}Th/^{230}Th atom ratio	2 s.e.	^{232}Th (pg/g)	2 s.e.	^{230}Th (fg/g)	2 s.e.	^{231}Pa	2 s.e.	(^{230}Th/^{231}Pa)	2 s.e.
A palmata	c2	2.806	0.005	146.7	0.7	12625	189	6785.0	17.3	532.8	4.3				
A cervicornis	Indian	2.912	0.005	145.3	0.8	—[b]		17.4	2.0	—[b]					
A formosa	c2	3.104	0.005	145.8	0.7	—		32.3	4.2	—					
Millepora	c1	0.321	0.001	146.5	0.7	—		27.0	4.1	—					
Tahiti	Pacific	2.157	0.003	146.0	0.7	—		86.0	4.8	—					
Bora Bora	Pacific	3.319	0.005	146.3	0.7	16036	464	5412.2	11.7	334.6	6.4				
Vanuatu	Pacific	3.107	0.005	145.1	0.7	8625	386	1540.1	14.2	177.0	4.2				
H tuna	c2	2.030	0.003	146.2	0.7	15074	630	2118.8	6.4	139.3	2.9				
H. tuna	c2 ash	2.147	0.003	146.0	0.8	14919	799	2172.5	35.3	145.1	4.3				
H. monile	c1	1.442	0.002	146.3	0.7	9902	266	3826.3	10.5	383.0	5.4				
H. monile	c1 ash	1.603	0.003	146.1	0.8	6624	116	2899.6	8.2	433.9	3.9				
Red algae	c1	0.536	0.001	148.3	0.7	8310	201	3351.2	9.0	399.8	4.9				
Red algae	c1 ash	0.613	0.001	147.7	0.8	7688	76	5449.2	13.7	702.7	3.9				
Ooids	c3	4.100	0.007	146.6	0.7	9170	36	47627.7	25.3	5149.1	41.0				
		Depth (m)	μg/kg					pg/kg		fg/kg		fg/kg			
01a	w1	6	3.434	0.006	146.2	1.0	25709	3008							
02a	w1	120	3.444	0.006	146.8	1.0	26174	3061	88.9	5.3	3.37	0.3	3.4	1.3	2.4	0.9
02b	w1	120	3.454	0.005	147.0	1.0	23434	2622	91.0	4.6	3.85	0.2	4.0	1.4	2.4	0.9
06a	w1	350	3.416	0.005	146.0	1.0	19732	1350	106.9	4.9	5.37	0.2	6.2	1.7	2.7	0.7
06b	w1	350	3.430	0.006	148.0	1.0	17314	1152	103.7	4.8	5.94	0.2	4.0	1.0	1.6	0.4
4	w1	430	3.404	0.005	146.7	1.0	13001	1060	97.6	4.8	7.44	0.3	1.7	1.0	0.5	0.3
07a	w1	580	3.411	0.007	146.6	1.0	13918	824	99.9	4.8	7.11	0.2	7.1	1.3	2.3	0.4
07b	w1	580	3.421	0.005	145.9	1.0	13925	1175	103.5	4.8	7.37	0.3	5.4	1.0	1.7	0.3
5	w1	950	3.374	0.005	147.4	1.0	17181	1638	93.0	4.9	5.37	0.3	4.5	1.2	1.9	0.5
3	w1	1650	3.457	0.005	146.0	1.0	24047	1836	103.1	4.7	4.25	0.2	4.3	1.3	2.3	0.7
Ex0	w2	0	3.484	0.006	146.6	1.2	24317	1913	96.6	4.8	3.94	0.2	5.3	1.0	3.1	0.6
Ex10	w2	10	3.469	0.005	146.4	1.0	25963	2018	100.6	4.9	3.84	0.2	4.8	1.0	2.9	0.6
Ex20	w2	20	3.472	0.005	146.6	1.0	31607	1930	136.7	5.0	4.29	0.2	5.4	1.1	2.9	0.6
Bank Top	w3	0	3.565	0.005	145.9	1.0	10477	676	91.9	4.8	8.70	0.3	0.5	—[c]	0.1	—[c]

[a] C1-3 are carbonate localities, and w1-3 are water-sampling localities (see Fig. 2). Carbonate samples labelled "ash" were ashed during chemical pretreatment, the others were heated in peroxide. ^{230}Th concentrations are corrected for ^{230}Th ingrowth during sample storage time. All errors are given as 2 s.e. and include the uncertainties detailed in the Section 4.4.

[b] ^{230}Th were close to the blank level of 25 fg when making carbonate measurements.

[c] ^{231}Pa was below the level of the blank so this value is not blank corrected. As a consequence the errors are large and the number is an upper bound on the true concentration.

centrations and isotope ratios (Fig. 5,Table 3). Corals have a ^{232}Th concentration from 0.017–6.79 ppb, algae from 2.12–5.45 ppb and ooids 47.63 ppb. The ^{232}Th/^{230}Th ratios range from 6500–15,000, corals from 8500–12,500 algae from 6500–15,500, and ooids at ~9200.

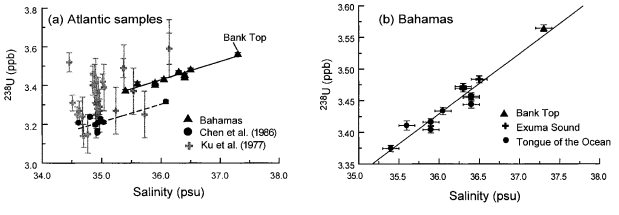

Fig. 4. U salinity measurements. (a) U-Salinity from the Bahamas (this study, triangles), and the Atlantic Ocean (Chen et al., 1986, circles; Ku et al., 1977, gray crosses). The solid line is the best-fit line through the Bahamas data and the dashed line is the best fit through the Chen et al. (1986) data. Both slopes have the same gradient but are slightly offset from one another. Data from this study indicate a seawater ^{238}U concentration of 3.33 ppb, normalized to a salinity of 35. (b) is an enlargement of (a) for the Bahamas measurements. Uncertainties for the U concentration are 2 s.e. and for salinity are 0.1.

Protactinium concentrations in the water column range from 1.7–7.1 fg/kg. Bank-top water has a very low concentration, at less than 0.5 fg/kg. In this study the errors are increased by the large contribution at 233 amu from abundance sensitivity (Sec-

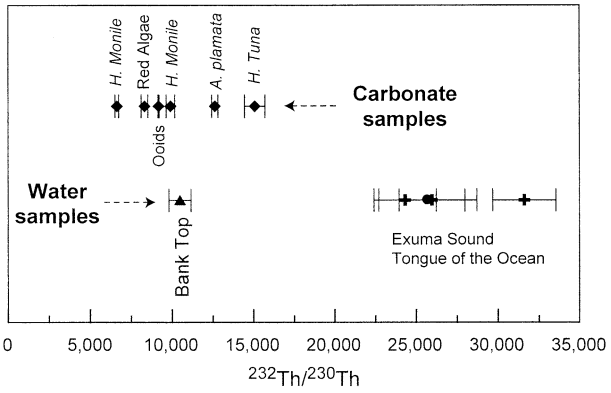

Fig. 5. ^{232}Th/^{230}Th ratios in Bahamas carbonates (as labeled) and surface waters from the bank top (triangle), Exuma Sound (crosses) and The Tongue of the Ocean (circles). All errors are 2 s.e.

tion 4.4 and Table 2). It will be straightforward to reduce this contribution by making a cleaner separation of uranium from the Th-Pa fraction since most of the interference is due to the tail of the ^{238}U. MC-ICP-MS will then offer a highly efficient method of ^{232}Th, ^{230}Th and ^{231}Pa analysis as the collection of each nuclide is maximized and chemical separation of Th from Pa is not required. In this study we believe that we have corrected ^{231}Pa measurements for abundance sensitivity accurately, but these corrections create large errors. Even with these errors, ^{231}Pa concentrations tend to be higher than previous open ocean ^{231}Pa values (e.g., Moran et al., 2001). Because of the problems with abundance sensitivity we hesitate to interpret this observation, but the general pattern of ^{231}Pa in the water column is robust, as any analytical problem will have affected all ^{231}Pa analyses in a similar way.

6. DISCUSSION

6.1. Incorporation of U and Th Isotopes in Marine Carbonates

U-Th dating of marine carbonates is a widely used technique that has yielded invaluable information in a range of areas, particularly in studies of Quaternary climate change (e.g., Edwards et al., 1986). When such dates are being calculated, it is important to know the initial U and Th isotope ratios.

The initial U isotope ratio, $\delta^{234}U_{initial,}$ is used to screen carbonates to test whether diagenesis has occurred since formation (Edwards et al., 1986). This approach requires that marine carbonates incorporate the same δ^{234}U value as seawater, and that seawater has a known δ^{234}U history. The latter issue has been discussed in the literature and δ^{234}U is thought not to have changed over the last few hundred thousand years (Gallup et al., 1994; Henderson, 2002). This study provides a more precise assessment of seawater δ^{234}U than previously available (Chen et al., 1986) and a precise test of the incorporation of this value into carbonates. Results demonstrate that seawater δ^{234}U averages 146.6 with a variation of $<$2.5‰, and that carbonates capture this value. The only possible exception is for red algae, which appear to have a slightly higher δ^{234}U of $\sim$148 (Fig. 1). In the other 12 samples of this study, including all the coral samples, there is no evidence for a higher initial δ^{234}U in carbonates than in seawater (Fig. 1), indicating the lack of very early diagenesis in the U/Th system.

Assessing the initial incorporation of Th isotopes is perhaps more important. The ingrowth of ^{230}Th from uranium forms the basis of the U/Th chronometer, so constraining the incorporation of initial ^{230}Th is a key issue. Corals are generally assumed to exclude thorium as they grow (Edwards et al., 1986) but even low concentrations of initial ^{230}Th in young corals can cause the resulting age to be inaccurate (e.g., Cobb et al., 2003). Initial ^{230}Th is more problematic in other types of carbonates, such as the aragonite sediments found in the Bahamas. Such sediments have been used to construct a detailed chronology of climate change in the Bahamas back to 240 ka (Slowey et al., 1996, Robinson et al., 2002), but this chronology relies on knowledge of the initial ^{230}Th concentration.

Initial ^{230}Th is often assessed by measuring the ^{232}Th concentration and assuming an initial ^{232}Th/^{230}Th. To use this approach for marine carbonates, it is necessary to know whether the initial ^{232}Th/^{230}Th directly reflects the seawater in which the carbonate formed, or whether the ratio differs through the incorporation or exclusion of detrital material with a higher ^{232}Th/^{230}Th ratio. Results from this study demonstrate that ooids and algal carbonates from the bank tops have very similar ^{232}Th/^{230}Th ratios to those of bank-top water from the same location (Fig. 5). Corals with sufficient Th to allow measurement of the ^{232}Th/^{230}Th ratio are from the edge of the bank and have values intermediate between normal surface water and bank-top water (Fig. 5). Carbonates therefore have thorium isotope ratios that reflect the seawater in which they grew. This result clearly shows that carbonates should not be corrected for initial ^{230}Th using detrital ^{232}Th/^{230}Th values, but that an assessment of the local seawater ^{232}Th/^{230}Th must be made and used for such a correction.

The coupled seawater and carbonate ^{232}Th measurements also allow calculation of the extent of thorium incorporation for each type of carbonate (expressed as a distribution coefficient, $[Th/Ca_{carb}]/[Th/Ca_{water}]$). These range from $\sim$0.2–70 for coral, to 25 for Halimeda, to as high as 500 for ooids. The high value for ooids is probably explained by their gradual formation process so that each layer is able to scavenge Th from seawater before it is covered by a new layer of calcite.

6.2. Conservative Nature of U Concentration

The ocean uranium cycle is thought to be close to steady state (Dunk et al., 2002) with a residence time of $\sim$400 kyr. Since the mean ocean-mixing time is much shorter than this residence time, uranium is expected to behave conservatively in seawater (e.g., Chen et al., 1986). If true, U concentrations should vary linearly with salinity. Previous attempts to confirm this have been hindered by the poor measurement precision of α-counting techniques (e.g., Ku et al., 1977; Fig. 4) or the small range in salinities measured by TIMS (Chen et al., 1986; Fig. 4). The high precision MC-ICP-MS analyses and large range of salinities of this study allow a reassessment of the U concentration-to-salinity relationship.

Previous studies have demonstrated nonconservative U behavior in certain environments. Flocculation of colloids where fresh and brackish waters mix can cause U draw-down (e.g., Porcelli et al., 1997). A change in oxidation state and hence solubility may cause either addition or removal of uranium (e.g., Barnes and Cochran, 1993). The Bahamas do not experience freshwater input and are fully oxic and so allow the conservative nature of uranium in the open ocean to be tested. The uranium-salinity relationship for samples analyzed in this study is seen to be linear over a salinity range of nearly 2 psu (with an R^2 value of 0.92), demonstrating the conservative behavior of U (Fig. 4). The U concentration at a salinity of 35 is 3.33 ppb, slightly higher than that reported in the Atlantic by Chen et al. (1986) (3.21 ppb, n = 10).

Results also demonstrate the constancy of δ^{234}U both with water depth and from ocean to ocean (Fig. 1). A simple box model verifies that we would expect the oceans to be well mixed with respect to δ^{234}U. If uranium with a δ^{234}U different by 800‰ is added to two ocean basins with a mixing time of 1000 yr and a uranium residence time of 400 kyr then the steady-state δ^{234}U difference between the oceans is $<$1‰. Despite this expectation, analytical confirmation of the oceanic

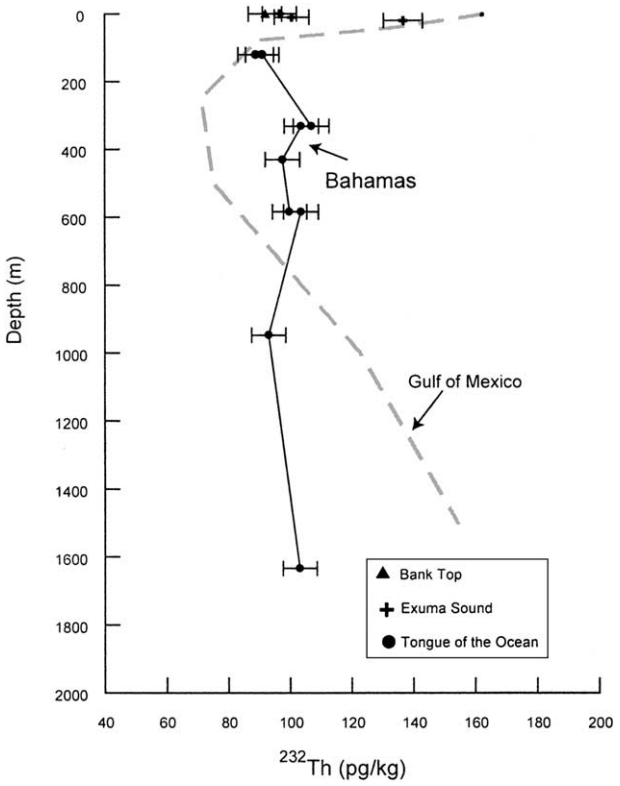

Fig. 6. ^{232}Th concentration (pg/kg) with depth. (To convert from pg/kg to dpm/1000 kg divide by 2.44×10^{-4}). Data are from the Bahamas (this study) and the Gulf of Mexico (Guo et al., 1995).

constancy of δ^{234}U is a reassuring result for the use of δ^{234}U both as a chronometer in its own right, and as a diagenetic check on U/Th ages.

6.3. What Controls Th and Pa in the Surface Waters of the Near-Shore Environment?

In contrast to uranium, both thorium and protactinium are extremely insoluble, with residence times of ~20 and ~100 yr respectively (Anderson et al., 1983). These short residence times make them very responsive to changes in environment, and the isotopes of Th and Pa have been used for a wide variety of purposes in the open ocean, including assessment of productivity and of ocean circulation. The behavior and uses of these isotopes in the near-shore and shelf environment has been less fully investigated, although both Th and particularly Pa are known to be preferentially removed from the oceans at their margins (Anderson et al., 1983). In this section we discuss the processes that control the concentrations of ^{232}Th, ^{230}Th, and ^{231}Pa in surface waters of the shelf environment.

6.3.1. Aeolian and riverine inputs

Terrestrial material with a high ^{232}Th concentration and ^{232}Th/^{230}Th ratio (~200,000) is added to the oceans as aeolian dust and by rivers (Figs. 6 and 7). Ocean regions close to riverine inputs frequently exhibit a surface maximum in ^{232}Th/^{230}Th due to injection of such riverine Th. For instance, surface water ^{232}Th/^{230}Th in the Hatteras and Nares Plains is 116,000 ± 22,000 and 205,000 ± 23,000 respectively (Cochran et al., 1987) reflecting riverine values ranging from 123,000 (Amazon) to 264,000 (Mississippi) (Scott, 1982). No such surface maximum is observed in the Bahamas water column, which is effectively cut off from riverine input by the Florida current. The only sources of ^{232}Th are advection from the north-east and dissolution of aeolian dust. Estimates of the dust input to the surface ocean in the region range from 1000 mg/m^2/yr (Andersen et al., 1998) to 5000 mg/m^2/yr (Duce et al., 1991). Assuming a dust ^{232}Th concentration of 13 ppm (Taylor S. R. and McLennan S. M., 1985) and a 100 m mixed layer, then the observed ^{232}Th concentration of ~100 pg/kg (Fig. 6) indicates a thorium residence time of 2–9 months in the mixed layer. This residence time is in good agreement with ^{234}Th-based estimates of surface-water Th residence times (Matsumoto, 1975) indicating that the ^{232}Th concentration of the surface waters can be readily explained by dust inputs.

6.3.2. Ingrowth in the water column

Surface water ^{232}Th/^{230}Th ratios are lower than those in dust because of the addition of ^{230}Th by U decay (Fig. 8). This ingrowth is most easily illustrated during laboratory storage and, indeed, must be corrected for in samples stored for long periods because the annual ingrowth of ~0.5 fg/kg ^{230}Th may be a significant portion of the original ^{230}Th concentration. In the surface ocean, with a residence time of up to 9 months, the ingrowth of ^{230}Th will be sufficient to reduce the ^{232}Th/^{230}Th ratio imparted by aeolian inputs by a factor of approximately two (i.e., from ~200,000 to 100,000). The measured surface water ^{232}Th/^{230}Th is significantly lower than this in the Bahamas (10,000–25,000) indicating an additional source of ^{230}Th to surface waters (see below).

6.3.3. Interaction with bank-top carbonates

An unusual feature of the Bahamas setting is the shallow water depths of the bank tops. The sediments therefore have a significant role in influencing the seawater Th and Pa isotope composition. Interaction between seawater and sediment is known to occur due to simple resuspension in nepheloid layers in some environments (Guo et al., 1995) but the role of sediment as a source or sink for these isotopes has otherwise not been assessed.

One striking observation is that waters on the bank tops have a significantly lower ^{232}Th/^{230}Th ratio (~10,000) than those immediately adjacent to the banks (24,000–31,000) (Fig. 7), despite the fact that bank-top waters are derived directly from these adjacent areas. Some mechanism on the bank tops is clearly able to alter the Th isotope ratio of the seawater. If this alteration were due solely to ^{230}Th ingrowth within the water column then the water would need to reside on the bank top for at least 10 yr—unrealistically long given that previous estimates of the maximum residence time is only 240 days, even in more isolated sections of the banks (Broecker and Takahashi, 1966; Morse et al., 1984). The change in isotope ratio must therefore relate to interaction with the sediment underlying the bank-top waters. Similarly, there is a marked difference between bank-top water (^{231}Pa/^{230}Th) and that in the adjacent

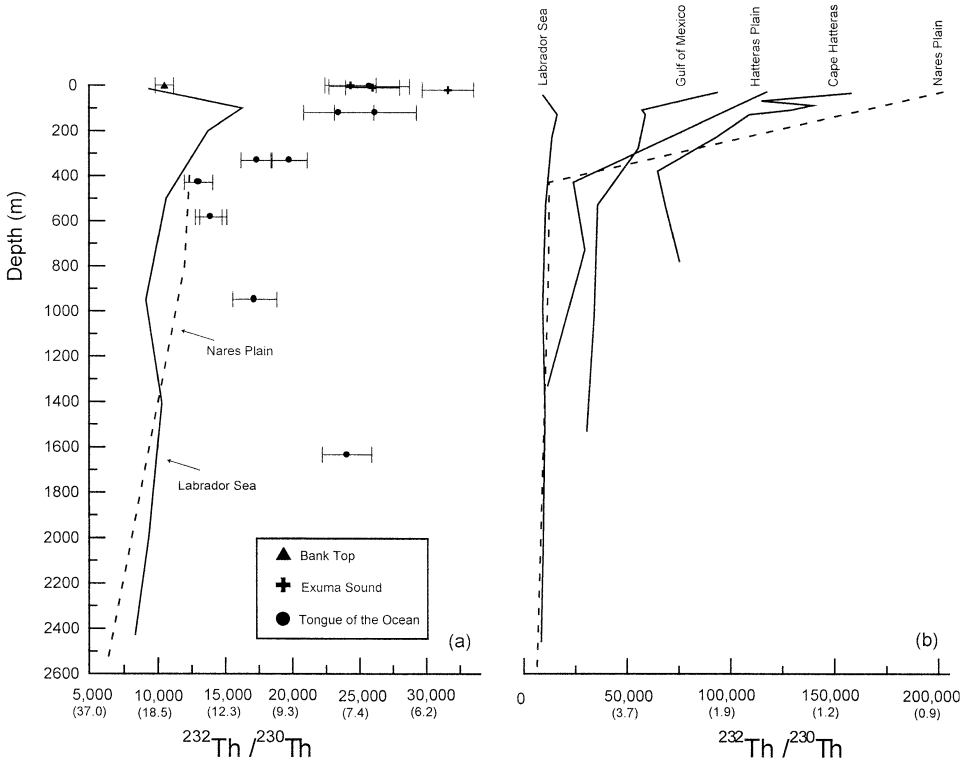

Fig. 7. $^{232}Th/^{230}Th$ ratios in water at 2 different scales. The x-axis shows $^{232}Th/^{230}Th$ atom ratios with ($^{230}Th/^{232}Th$) activity ratios in parentheses. Circles are from the TOTO (w1), crosses are from Exuma Sound (w2) and triangles are from the bank top (w3). All errors are 2 s.e. For comparison $^{232}Th/^{230}Th$ from the Labrador Sea (Moran et al., 1997), Cape Hatteras, Gulf of Mexico (Guo et al., 1995), Nares Plain (dashed line) and the Hatteras Plain (both from Cochran et al., 1995).

seas, again suggesting a role for sediment interaction in setting the seawater isotope composition (Fig. 9).

The most likely interaction would be addition of ^{230}Th and ^{231}Pa by α-recoil from the underlying carbonate sediment. Alpha-recoil is the process by which a radioactive daughter is mobilized from its initial position by the energy of alpha decay ($\sim$ 4–9 MeV). The length scale is on the order of 10^{-8}–10^{-7} m, so only those nuclides that are near the edge of the grain are in a position to be ejected directly (Kigoshi, 1971).

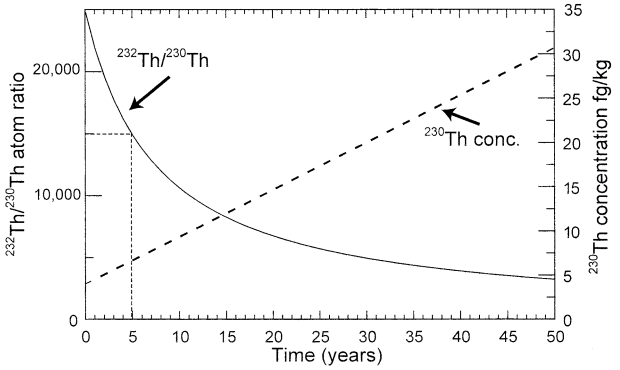

Fig. 8. Evolution of thorium isotopes in an isolated water body with time assuming a ^{238}U concentration of 3.5 ppb, a $\delta^{234}U$ of 146, a ^{232}Th concentration of 100 pg/kg and an initial ^{230}Th concentration of 4 fg/kg. The solid line is the $^{232}Th/^{230}Th$ atom ratio and the dashed line is the ^{230}Th concentration in fg/kg. This plot clearly demonstrates that it is necessary to correct measured values for ingrowth of ^{230}Th since sample collection. Approximately 0.5 fg/kg/yr of ^{230}Th grows in 1 yr, some 10% of the surface water concentration.

To test the viability of α-recoil as an important process in setting the bank-top seawater chemistry we use a simple box model approach (Fig. 10). In this model, we start by considering ^{232}Th, which is not affected by recoil. Inputs of ^{232}Th to the bank top are aeolian dust and water flowing onto the banks. This input must be balanced by waters flowing off the banks and by removal of ^{232}Th to the sediments forming on the bank top. Assuming a plausible residence-time for waters on the bank top of $\sim$0.4 yr, the ^{232}Th balance suggests that $\sim$94% of the ^{232}Th added to the bank top by dust and advection is removed to the sediment. For the other Th isotope, ^{230}Th, 94% removal of the dust and advection inputs is therefore also expected. With this level of removal, an additional source of ^{230}Th is required to provide the ^{230}Th that leaves the banks by advection. This additional source of ^{230}Th is likely to be alpha recoil from the sediment, and the magnitude of this recoil flux can readily be calculated from the mass balance (Fig. 10). Making the reasonable assumption that the ^{231}Pa recoil rate is related to the ^{230}Th recoil rate by the production ratio of these two nuclides, a ^{231}Pa budget can also be calculated for the bank tops. This suggests a rather similar extent of Pa ($\sim$91%) and Th ($\sim$94%) removal. As expected, Th is scavenged to a greater

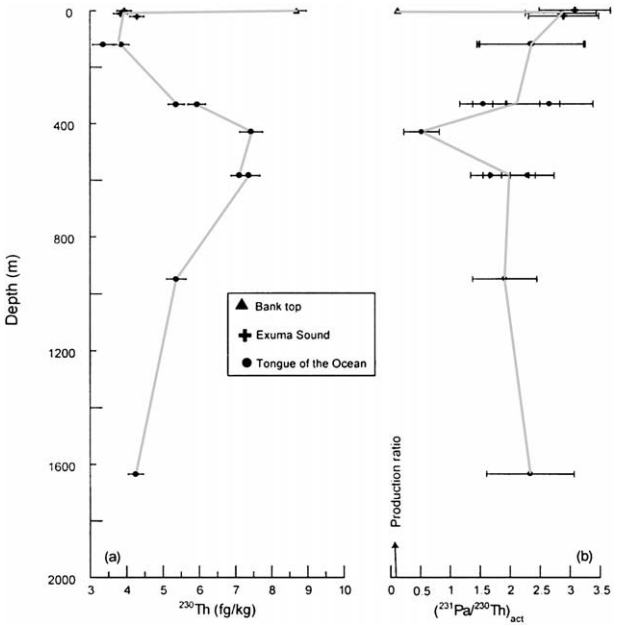

Fig. 9. (a) ^{230}Th (fg/kg) and (b) (^{231}Pa/^{230}Th) in the water column. Error bars are 2 s.e. and are shown for all samples except bank top (^{231}Pa/^{230}Th) where the ^{231}Pa concentration is a maximum value.

extent than Pa. However, the nearly complete removal of both these isotopes from the water column results in the scavenging ratio being closer to unity than may be expected from an open-ocean perspective. In summary, this box model indicates that it is indeed possible to explain the dramatic change observed in ^{232}Th/^{230}Th and (^{231}Pa/^{230}Th) on the bank tops by almost quantitative removal of Th and Pa by scavenging, and their replacement with a mixture of recoil ^{230}Th and ^{231}Pa, and dust ^{232}Th (Fig. 10).

From a sedimentary perspective, this amount of recoil ^{230}Th is reasonable. The flux of ^{230}Th required is generated in only an 11 cm thick layer of Bahamas sediment (with a typical U concentration of 3.5 ppm). Only a fraction of this ^{230}Th is expected to be recoiled to the water, but the strong bank-top currents cause pore fluid flow to a significant depth in the sediment. It is therefore reasonable that the U-rich carbonate sediments label water that resides on the bank top with a low ^{232}Th/^{230}Th value and a (^{231}Pa/^{230}Th) close to the production ratio (0.093). In the open-ocean, preferential scavenging of ^{230}Th causes (^{231}Pa/^{230}Th) to be greater than the production ratio (e.g., ~0.4 for the Equatorial Atlantic; Moran et al., 2001). The production ratio values observed on the bank top are therefore very characteristic and provide the possibility of tracing this water once it leaves the banks.

There is no doubt that the Bahama Banks are particularly sensitive to the effects of this sediment-water interaction due to the large expanse of shallow water and the time that water remains on the bank tops. Similar processes are likely to occur at other sediment-water interfaces, but may be masked by the effect of rapid advection and diffusion of the waters away from the sediment. These α-recoil effects may, however, also be observable in shallow shelf environments and might label these shelf waters in a similar manner to the Bahamas bank-top waters studied here. In other areas such effects will be overwhelmed by input of crustal ^{232}Th from the continents, but in that case, shelf waters are still expected to be labeled with a Th isotope composition different from open ocean seawater.

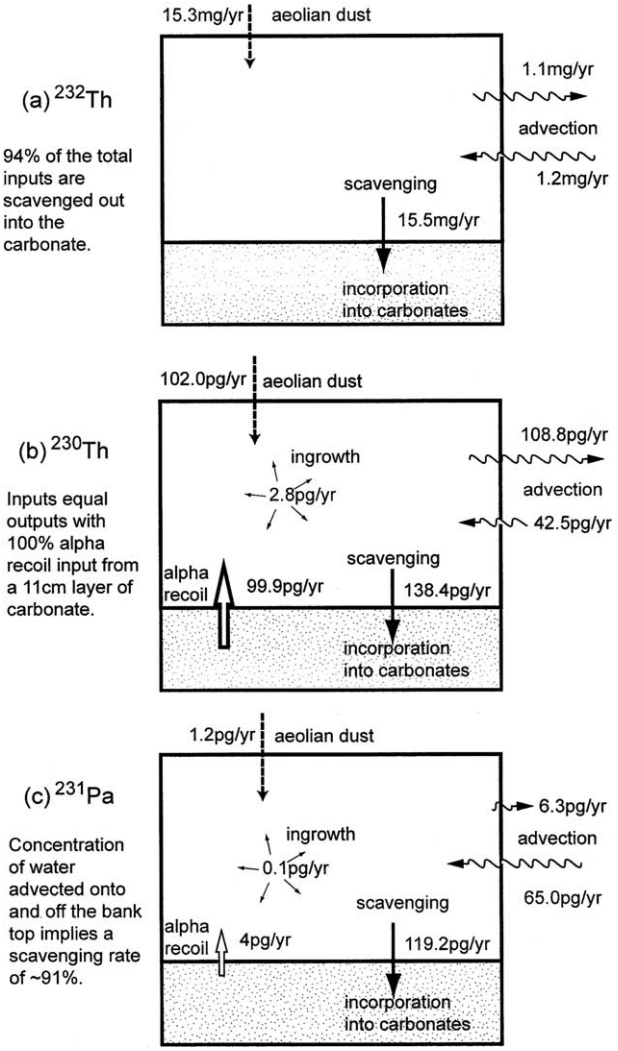

Fig. 10. Bank-top model for (a) ^{232}Th, (b) ^{230}Th and (c) ^{231}Pa budgets. The model suggests that >90% of all the Th and Pa are scavenged out into the underlying carbonates. (a) ^{232}Th is added to the bank top by dust and water advection. It is removed by scavenging and water advection. An aragonite production rate of 500 g/m^2/yr (Broecker and Takahashi, 1966) and an average carbonate ^{232}Th concentration of 31 ng/g (60% ooids, 40% Halimeda) implies that ~15.5μg/yr ^{232}Th are removed into sediments. ^{232}Th is being added to the surface ocean by aeolian dust at a rate between 13 and 65μg/yr. A simple mass balance of inputs (aeolian dust and advection) and outputs (scavenging and advection) allows us to calculate a water residence time of 0.4 yr and a dust input of 15.3μg/yr. This level of incorporation implies that ~94% of the thorium that enters the bank-top system is scavenged out of the water column into the sediments. (b) ^{230}Th has two additional inputs: ingrowth from U decay in the water column; and α-recoil input from the sediments. If ~94% of this ^{230}Th is scavenged out as for ^{232}Th, then 100 pg/yr must be added by alpha recoil to balance the ^{230}Th budget. (c) The combined contributions of advection (65 pg/yr), aeolian dust (1.2 pg/yr, assuming 3 ppm ^{238}U and secular equilibrium), ingrowth in the water column (0.1 pg/yr) and alpha recoil (4 pg/yr, assuming recoil at the (^{231}Pa/^{230}Th) production ratio) give a total ^{231}Pa input of 70 pg/yr. Only 6 pg/yr are advected off the bank top implying that ~91% of Pa is scavenged into the underlying sediments.

6.4. Using U-Series Isotopes as Near-Shore Water Mass Tracers

In this section we use $^{232}Th/^{230}Th$ and ($^{231}Pa/^{230}Th$) to investigate ocean circulation in the Bahamas environment. In an open-ocean situation with no advection, we would expect $^{232}Th/^{230}Th$ to decrease monotonically with depth in the water column as ^{230}Th forms from decay and is transported down the water column by scavenging. In the Bahamas profile this is not the case and there is, instead, a clear minimum in $^{232}Th/^{230}Th$ at 430 m (Fig. 7). This minimum in the Bahamas requires either a source of high $^{232}Th/^{230}Th$ at depth or of low $^{232}Th/^{230}Th$ at 430 m.

First, we will consider mechanisms that may increase $^{232}Th/^{230}Th$ at depth. A dramatic rise in the ratio is often seen at the base of water profiles where sediment is resuspended. The increase in $^{232}Th/^{230}Th$ in this study cannot be due to such entrained sediment for two reasons: the total water depth is significantly greater than 1650 m and there is no associated increase in ^{232}Th concentration. A second possible source of high $^{232}Th/^{230}Th$ values at depth is the Caribbean Sea. Guo et al. (1995) present a depth profile from the Gulf of Mexico which has $^{232}Th/^{230}Th$ of >35,000 down to 1,500 m (Fig. 7). Slowey and Curry (1995), however, show that water in the Providence channels comes not from the Caribbean Sea but from the opposite direction—the Sargasso Sea. The Bahamas are effectively cut off from the Caribbean Sea by the Straits of Florida, and Caribbean source water is therefore not a viable source.

Mechanisms to explain the high $^{232}Th/^{230}Th$ at depth do not seem plausible, so we turn instead to an explanation for the low $^{232}Th/^{230}Th$ at ~430 m. An obvious source of water with such low $^{232}Th/^{230}Th$ is from the bank top (Figs. 9 and 10). The isotope ratio at 430 m indicates a 65–75% proportion of bank-top water. This mechanism to explain the minimum in $^{232}Th/^{230}Th$ is supported by the ($^{231}Pa/^{230}Th$) profile that also shows a distinct deviation to low values, similar to those observed on the bank top, at this depth (Fig. 9).

Density cascading of hyperpycnal water has previously been observed and is described by several authors (Wilson and Roberts, 1992, 1995; Wilber et al., 1993). Wilson and Roberts (1995) suggest that during a cold front, bank-top waters reach peak density as cold dry air causes intense evaporation, increasing salinity and cooling the waters. This water cascades off the side of the bank, resuspending sediment and reaching depths as great as 800 m, but more generally ~500 m. Such density cascading events might explain the Th and Pa isotope ratios seen at 430 m in two ways. First, the water may itself be dense due to cooling of the already saline bank-top waters (Wilson and Roberts, 1992, 1995). The bank-top waters would sink to a depth of neutral buoyancy at 400–500 m to explain the low $^{232}Th/^{230}Th$ and ($^{231}Pa/^{230}Th$) observed at that depth. In this case, a temperature-salinity (T-S) signal of bank-top waters would also be expected at 430 m. Salinity measurements at this depth do indeed show a small salinity increase, but this is barely resolvable and is insufficient to indicate the presence of bank-top water (Fig. 11). This result suggests that sediment-loaded density cascading may dominate. In this mechanism the bank-top waters are made dense due to both their T-S characteristics and to addition of sediment particles. Through active exchange, this sediment would label water at 430 m with a bank-top $^{232}Th/^{230}Th$ and ($^{231}Pa/^{230}Th$) signal without requiring a dramatic increase in salinity (Fig. 12).

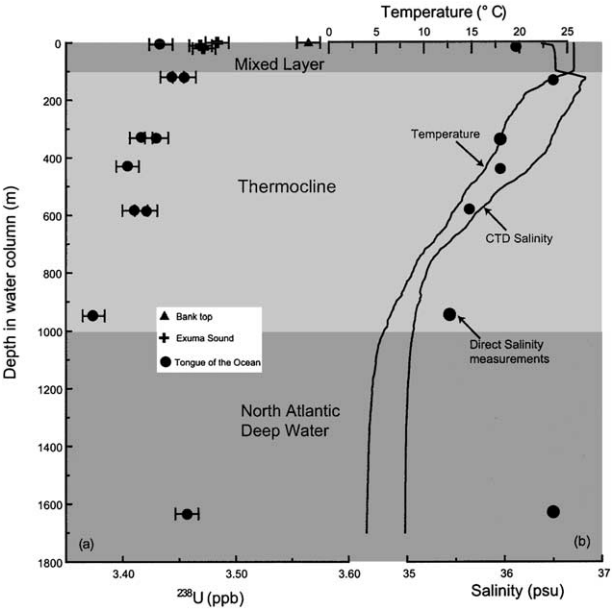

Fig. 11. (a) Concentration of ^{238}U with depth in the water column. Circles are from the TOTO (w1), crosses are from Exuma Sound (w2) and the triangle is from the bank top (w3) (see Fig. 2 for locations). All errors are 2 s.e. (b) CTD data showing salinity and temperature taken at 25.761°N, 77.412°W (data supplied by Niall Slowey; Slowey and Curry, 1995). Direct salinity measurements made on waters recovered from the TOTO profile are shown as circles, with a precision of 0.1.

The example of the Bahamas suggests that Th and Pa may be useful proxies to investigate local circulation features in other near-shore environments. Wherever surface waters are labeled with a high $^{232}Th/^{230}Th$ ratio through terrestrial inputs, or a low $^{232}Th/^{230}Th$ through recoil processes, this ratio might prove useful to follow the water mass once it leaves the surface.

7. CONCLUSIONS

Modern carbonates from the Bahamas bank top have the same $^{232}Th/^{230}Th$ and $\delta^{234}U$ as bank-top waters. The fact that modern carbonates incorporate the U and Th isotopes of the local seawater in which they form supports the assumptions inherent in U-Th dating of Quaternary carbonates. Water in shallow bank or shelf environments is greatly influenced by the underlying sediment. Both ^{230}Th and ^{231}Pa can be added by alpha recoil and removed by scavenging. The result of this interaction is to allow water to be labeled rapidly with distinctive isotopic signatures. This labeling allows both $^{232}Th/^{230}Th$ and ($^{231}Pa/^{230}Th$) to be used to trace the movement of water in the Bahamas. These tracers show that water sinks from the bank top to a depth of neutral buoyancy at ~ 430 m, supporting the mechanism of density cascading for moving sediment to the slopes of the Bahamas Banks. The advances in Th, Pa and U isotope analysis using multiple ion counters will enable small water samples to be measured on a routine basis. Th and Pa isotopes will therefore be well suited to the study of oceanographic processes in shallow water regions.

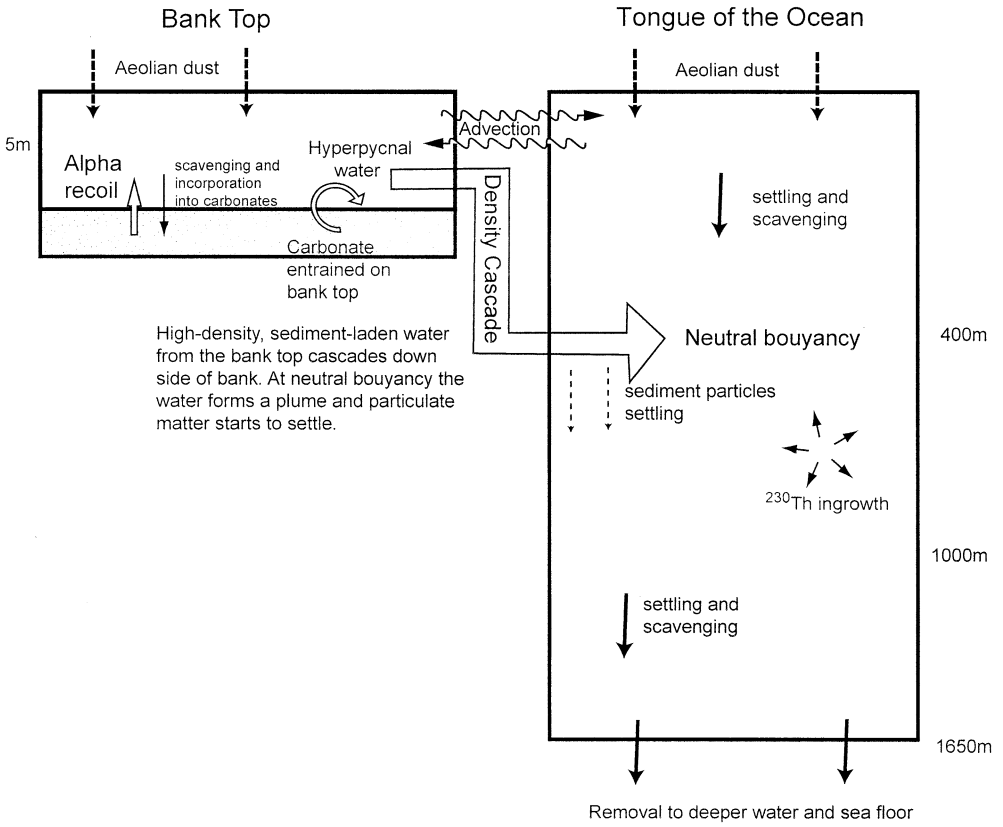

Fig. 12. Model to show the mechanisms affecting Th and Pa in the Bahamas. At all times dust is being added to the surface and ^{230}Th and ^{231}Pa are growing by decay from uranium. Bank-top water and carbonates are in equilibrium with one another labeling bank-top waters with a distinctive signature. As dense bank-top water moves off the bank it entrains sediment before it flows down the slope to a depth of neutral buoyancy. At this depth the sediment settles out leaving the water with a bank-top label.

Acknowledgments—This research was supported by NERC research studentship GT/04/99/ES/208 and a CASE from Nu Instruments to LFR, and by NERC grant GR3/12828. Niall Slowey is thanked for the CTD data. Modern coral samples were collected by El Breman, Eleanor James and Nicky White. Simon Turner and Kia Rostami at Bristol University produced the ^{233}Pa spike. Many thanks to the crew on the Calanus and the staff at CMRC for their help in making field work not only a success but a pleasure. We are grateful for the comments of Dr. Lee Kump, Professor S. J. Goldstein and three anonymous reviewers which greatly improved the manuscript.

Associate editor: L. R. Kump

REFERENCES

Andersen K. K., Armengaud A., and Genthon C. (1998) Atmospheric dust under glacial and interglacial conditions. *Geophys. Res. Lett.* **25,** 2281–2284.

Anderson R. F., Bacon M. P., and Brewer P. G. (1983) Removal of ^{230}Th and ^{231}Pa at ocean margins. *Earth Planet. Sci. Lett.* **66,** 73–90.

Anderson R. F., Lao Y., Broecker W. S., Trumbore S. E., Hofmann H. J., and Wolfli W. (1990) Boundary scavenging in the Pacific Ocean: A comparison of ^{10}Be and ^{231}Pa. *Earth Planet. Sci. Lett.* **96,** 287–304.

Andersson Per S., Wasserburg G. J., Chen J. H., Papanastassiou D. A., and Ingri J. (1995) ^{238}U-^{234}U and ^{232}Th-^{230}Th in the Baltic Sea and in river water. *Earth Planet. Sci. Lett.* **130,** 217–234.

Bacon M. and Anderson R. (1982) Distribution of thorium isotopes between dissolved and particulate forms in the deep sea. *J. Geophys. Res.* **87 (***C3***),** 2045–2056.

Banner J. L., Wasserburg G. J., Chen J. H., and Moore C. H. (1990) ^{234}U-^{238}U-^{230}Th-^{232}Th systematics in saline groundwaters from central Missouri. *Earth Planet. Sci. Lett.* **101,** 296–312.

Barnes C. E. and Cochran J. K. (1993) Uranium geochemistry in estuarine sediments; controls on removal and release processes. *Geochim. Cosmochim. Acta* **57,** 555–569.

Belshaw N. S., Freedman P. A., O'Nions R. K., Frank M., and Guo Y. (1998) A new variable dispersion double-focusing plasma mass spectrometer with performance illustrated for Pb isotopes. *Int. J. Mass Spectrom.* **181,** 51–58.

Broecker W. S. and Takahashi T. (1966) Calcium carbonate precipitation on the Bahama Banks. *J. Geophys. Res.* **71,** 1575–1602.

Chen J. H., Edwards R. L., and Wasserburg G. J. (1986) ^{238}U^{234}U and ^{232}Th in seawater. *Earth Planet. Sci. Lett.* **80,** 241–251.

Chen J. H., Curran H. A., White B., and Wasserburg G. J. (1991) Precise chronology of the last interglacial period: ^{234}U-^{230}Th data from fossil coral reefs in the Bahamas; with supplemental data 91–01. *Geol. Soc. Am. Bull.* **103,** 82–97.

Cheng H., Edwards R. L., Hoff J., Gallup C. D., Richards D. A., and Asmeron Y. (2000a) The half-lives of ^{234}U and ^{230}Th. *Chem. Geol.* **169,** 17–33.

Cheng H., Adkins J., Edwards R. L., and Boyle E. A. (2000b) U-Th dating of deep-sea corals. *Geochim. Cosmochim. Acta* **64,** 2401–2416.

Choi M. S., Francois R., Sims K., Bacon M. P., Brown-Leger S., Fleer A. P., Ball L., Schneider D., and Pichat S. (2001) Rapid determination of ^{230}Th and ^{231}Pa in seawater by desolvated micro-nebulization inductively coupled plasma mass spectrometry. *Mar. Chem.* **76,** 99–112.

Cobb M. M., Charles D. D., Cheng H., Kastner M., and Edwards R. L. (2003) U/Th-dating living and young corals from the central tropical Pacific. *Earth Planet. Sci. Lett.* **210,** 91–103.

Cochran J. K., Livingston Hugh D., Hirschberg David J., and Surprenant Lolita D. (1987) Natural and anthropogenic radionuclide distributions in the Northwest Atlantic Ocean. *Earth and Planetary Science Letters* **84**(2–3), 135–152.

Cochran J. K., Hirschberg D. J., Livingston H. D., Buesseler K. O., Key R. M., and Livingston H. D. (1995) Natural and anthropogenic radionuclide distributions in the Nansen Basin, Arctic Ocean: Scavenging rates and circulation timescales. *Deep-Sea Res. II* **42,** 1495–1517.

Duce R. A., Liss P. S., Merrill J. T., Atlas E. L., Buat-Menard P., Hicks B. B., Miller J. M., Prospero J. M., Arimoto R., Church T. M., Ellis W., Galloway J. N., Hansen L., Jickells T. D., Knap A. H., Reinhardt K. H., Schneider B., Soudine A., Tokos J. J., Tsunogai S., Wollast R., and Zhou M. (1991) The atmospheric input of trace species to the world ocean. *Global Biogeochem. Cycles* **5,** 193–259.

Dunk R. M., Mills R. A., and Jenkins W. J. (2002) A reevaluation of the oceanic uranium budget for the Holocene. *Chem. Geol.* **190,** 45–67.

Edwards R. L., Chen J. H., and Wasserburg G. J. (1986) ^{238}U-^{234}U-^{230}Th-^{232}Th systematics and the precise measurement of time over the past 500 000 years. *Earth Planet. Sci. Lett.* **81,** 175–192.

Gallup C. D., Edwards R. L., and Johnson R. G. (1994) The timing of high sea levels over the past 200,000 years. *Science* **263 (***5148***),** 796–800.

Guo L., Santschi P. H., Baskaran M., and Zindler A. (1995) Distribution of dissolved and particulate ^{230}Th and ^{232}Th in seawater from the Gulf of Mexico and off Cape Hatteras as measured by SIMS. *Earth Planet. Sci. Lett.* **133,** 117–128.

Henderson G. M., Slowey N. C., and Haddad G. A. (1999) Fluid flow through carbonate platforms: Constraints from ^{234}U/^{238}U and Cl^- in Bahamas pore-waters. *Earth Planet. Sci. Lett.* **169,** 99–111.

Henderson G. M., Slowey N. C., and Fleisher M. Q. (2001) U-Th dating of carbonate platform and slope sediments. *Geochim. Cosmochim. Acta* **65,** 2757–2770.

Henderson G. M. (2002) Seawater (^{234}U/^{238}U) during the last 800 thousand years. *Earth and Planetary Science Letters* **199**(1–2), 97–110.

Henderson G. M. and Anderson R. F. (2003) The U-series toolbox for paleoceanography. *Rev. Mineral. Geochem.* **52,** 493–531.

Hickey B. M., MacCready P., Elliott E., and Kachel N. B. (2000) Dense saline plumes in Exuma Sound, Bahamas. *J. Geophys. Res. C* **105,** 11,471–11,488.

Kigoshi K. (1971) Alpha-recoil thorium-234; dissolution into water and the uranium-234/uranium-238 disequilibrium in nature. *Science* **173 (***3991***),** 47–48.

Ku T. L., Knauss K. G., and Mathieu G. G. (1977) Uranium in open ocean; concentration and isotopic composition. *Deep-Sea Res.* **24,** 1005–1017.

Lazar B., Stein M., Enmar R., Bar-Matthews M., and Halicz L. (2002) The effect of diagenesis on the U system in live and Holocene coral from the Red Sea. *Geochim. Cosmochim. Acta* **66 (***15A Suppl. 1***),** A436.

Ludwig K. R., Szabo B. J., Moore J. G., and Simmons K. R. (1991) Crustal subsidence rate off Hawaii determined from ^{234}U/^{238}U ages of drowned coral reefs. *Geology* **19,** 171–174.

Ludwig K. R. and Paces J. B. (2002) Uranium-series dating of pedogenic silica and carbonate, Crater Flat, Nevada. *Geochim. Cosmochim. Acta* **66,** 487–506.

Luo X., Rehkämper M., Der-Chuen L., and Halliday A. N. (1997) High precision ^{230}Th/^{232}Th and ^{234}U/^{238}U measurements using energy filtered ICP magnetic sector multiple collector mass spectrometry. *Int. J. Mass Spectrom. Ion Processes* **171,** 105–117.

Matsumoto E. (1975) ^{234}Th-^{238}U radioactive disequilibrium in the surface layer of the oceans. *Geochim. Cosmochim. Acta* **39,** 205–212.

Moran S. B., Charette M. A., Hoff J. A., Edwards R. L., and Landing W. M. (1997) Distribution of ^{230}Th in the Labrador Sea and its relation to ventilation. *Earth Planet. Sci. Lett.* **150,** 151–160.

Moran S. B., Shen C.-C., Weinstein L. H., Hettinger L. H., Hoff J. H., Edmonds H. N., and Edwards R. L. (2001) Constraints on deep water age and particle flux in the South Atlantic Ocean based on seawater ^{231}Pa and ^{230}Th data. *Geophys. Res. Lett.* **28,** 3437–3440.

Morse J. W., Millero F. J., Thurmond V., Brown E., and Ostland H. G. (1984) The carbonate chemistry of Grand Bahama Bank waters: After 18 years another look. *J. Geophys. Res.* **89 (***C3***),** 3604–3614.

Nozaki Y. and Yamada M. (1987) Thorium and protactinium isotope distributions in waters of the Japan Sea. *Deep-Sea Res. A* **34,** 1417–1430.

Nozaki Y. and Yang H. S. (1987) Th and Pa isotopes in the waters of the western margin of the Pacific near Japan: Evidence for release of ^{228}Ra and ^{227}Ac from slope sediments. *J. Oceanogr. Soc. Jpn.* **43,** 217–227.

Nozaki Y., Yang Hang S., and Yamada M. (1987) Scavenging of thorium in the ocean. *J. Geophys. Res. C* **92,** 772–778.

Pietruszka A. J., Carlson R. W., and Hauri E. H. (2002) Precise and accurate measurements of ^{226}Ra ^{230}Th and ^{238}U disequilibria in volcanic rocks using plasma ionization multicollector mass spectrometry. *Chemical Geology* **188,** 171–191.

Porcelli D., Andersson Per S., Wasserburg G. J., Ingri J., and Baskaran M. (1997) The importance of colloids and mires for the transport of uranium isotopes through the Kalix River watershed and Baltic Sea. *Geochim. Cosmochim. Acta* **61,** 4095–4113.

Robinson L. F., Henderson G. M., and Slowey N. C. (2002) U-Th dating of marine isotope stage 7 in Bahamas slope sediments. *Earth Planet. Sci. Lett.* **196,** 175–187.

Roy-Barman M., Chen J. H., and Wasserburg G. J. (1996) ^{230}Th-^{232}Th systematics in the Central Pacific Ocean: The sources and the fates of thorium. *Earth Planet. Sci. Lett.* **139,** 3–4.

Scott M. R. (1982) The chemistry of U and Th nuclides in rivers. In *Uranium Series Disequilibrium: Applications to Environmental Problems* (eds. M. Ivanovich and R. S. Harmon), pp. 181–201. Clarendon Press.

Shen C. C., Edwards R. L., Cheng H., Dorale J. A., Thomas R. B., Moran S. B., Weinstein S. E., and Edmonds H. N. (2002) Uranium and thorium isotopic and concentration measurements by magnetic sector inductively coupled plasma mass spectrometry. *Chem. Geol.* **185,** 165–178.

Slowey N. C. and Curry W. B. (1995) Glacial-interglacial differences in circulation and carbon cycling within the upper western North Atlantic. *Paleoceanography* **10,** 715–732.

Slowey N. C., Henderson G. M., and Curry W. B. (1996) Direct U-Th dating of marine sediments from the two most recent interglacial periods. *Nature* **383 (***6597***),** 242–244.

Stirling C. H., Esat T. M., Lambeck K., McCulloch M. T., Blake S. G., Lee D. C., and Halliday A. N. (2001) Orbital forcing of the marine isotope stage 9 interglacial. *Science* **291 (***5502***),** 290–293.

Szabo B. J., Ludwig K. R., Muhs D. R., and Simmons K. R. (1994) Thorium-230 ages of corals and duration of the last interglacial sea-level high stand on Oahu, Hawaii. *Science* **266 (***5182***),** 93–96.

Taylor S. R. and McLennan S. M. (1985) *The Continental Crust: Its Composition and Evolution*. Blackwell Scientific.

Whitaker F. F. and Smart P. L. (1990) Active circulation of saline ground waters in carbonate platforms; evidence from the Great Bahama Bank. *Geology* **18,** 200–203.

Wilber R. J., Whitehead J. A., Halley R. B., and Milliman J. D. (1993) Carbonate-periplatform sedimentation by density flows; a mechanism for rapid off-bank and vertical transport of shallow-water fines: Comment. *Geology* **21,** 667–668.

Wilson P. A. and Roberts H. H. (1992) Carbonate-periplatform sedimentation by density flows; a mechanism for rapid off-bank and vertical transport of shallow-water fines. *Geology* **20,** 713–716.

Wilson P. A. and Roberts H. H. (1993) Carbonate-periplatform sedimentation by density flows; a mechanism for rapid off-bank and vertical transport of shallow-water fines: Reply. *Geology* **21,** 668–669.

Wilson P. A. and Roberts H. H. (1995) Density cascading; off-shelf sediment transport, evidence and implications, Bahama Banks. *J. Sediment. Res. A* **65,** 45–56.